

ELECTRIC FIELD INDUCED RESISTANCE SWITCHING AND MAGNETIC SWITCHING PROPERTIES OF Fe₇₀Ga₃₀ NANO THIN FILMS

H. LI*, Y. M. HAN, X. M. REN, Z. TAO, K. L. ZHANG

School of Electrical and Electronic Engineering, Tianjin Key Laboratory of Film Electronic & Communication Devices, Tianjin University of Technology, Tianjin 300384, China

Fe₇₀Ga₃₀ magnetic nano thin films of different thicknesses were successfully fabricated by ion beam deposition coating on Si/SiO₂ substrates. The crystal structure of Fe₇₀Ga₃₀ magnetic nano thin films were characterized by Grazing incidence X-ray diffraction (GIXRD). Surface morphology is studied using Atomic Force Microscopy (AFM). The magnetic properties of nano thin films have been measured by Vibrating Sample Magnetometer (VSM). The result reveals that the nano thin films have good soft magnetic properties. We measured the current–voltage (I–V) curves of Fe₇₀Ga₃₀ nano thin films, the behavior of resistance switching by more than an order of magnitude was obtained. The measurement performed on Fe₇₀Ga₃₀ nano thin films reveal that the resistant switching behavior is reversible and the transformation occurs between high (low) resistance states. The manipulation could be attributed to the Coulomb blockade effect. The existence of anomalous Hall effect was found during the Hall effect test on the nano thin films surface. The surface carrier density of Fe₇₀Ga₃₀ nano thin films changed when Hall effect test was performed resulting in magnetic switching.

(Received December 19, 2019; Accepted April 15, 2020)

Keywords: Magnetic nano thin films, Resistance switching, Coulomb blockade effect, Anomalous Hall effect, Magnetic switching

1. Introduction

In a recent study, Spaldin N et al. described the possibility of using electric fields to directly regulate the magnetic properties of magnetic materials [1]. In experimental work, Martin Weisheit et al. studied the modulation of the magnetic properties of ultra-thin FePt and FePd by an electric field. By adjusting the density of unpaired d electrons near the Fermi level of the metal film, the magnetic crystal anisotropy of ferromagnetic films is also modulated. The experimental results show that the voltage change of 0.6mV will cause the coercivity of FePt and FePd alloys with a thickness of 2nm to decrease by 4.5% and increase by 1%. This is the first experimental work to observe the electric field directly regulating the magnetic properties of metal thin films [2]. Since then, Wulfhekel et al. obtained the magnetoelectric effect in metallic magnetic materials. They used an electric field to change the electronic structure of the Fe film with a thickness of

* Corresponding author: 740293354@qq.com

several atomic layers to change the resistance of the Fe film, indicating that the magnetic properties can be achieved without an insulating layer. The electrical coupling effect can be used to construct a metal non-volatile memory using the electromagnetic change of the Fe film [3]. Maruyama T et al. In the Au / Fe (several atomic layer) / MgO / polyimide / ITO structure used a small electric field of 45mV / nm to produce significant changes in magnetic anisotropy, which is low for spin electron devices Significance of writing power information [4]. In the Fe/MgO structure with only a few atomic layer thickness body-centered cubic Fe films, the change in magnetic anisotropy can be significantly induced by using an electric field. This is mainly by using the electric field to change the 3d orbital arrangement. The applied electric field Changed Fermi level and affected the electronic arrangement of different orbits, and the macroscopic magnetism changed accordingly [5].

Ferromagnetic metals and some of their alloys have a Curie temperature higher than room temperature, and direct modulation of magnetic properties using an electric field is of great significance for the realization of new memory devices [6]. However, due to the electrostatic shielding phenomenon of metal under the action of an electric field, the induced charge on the metal surface will prevent the electric field from entering the conductor, and the electric field can only exist on the atomic scale of the surface [7]. Therefore, in ultra-thin ferromagnetic metal thin films, the electric field may modulate the carrier density and electron arrangement of the metal thin film. Unpaired d electrons close to the Fermi level in the 3d metal can act as free carriers to regulate the surface charge, thereby realizing the modulation of the macroscopic magnetic properties by the electric field [8].

For 3d metals and alloys such as Fe, Co, and Ni, the change in carrier density directly affects the magnetic crystal anisotropy and its corresponding energy [9]. FeGa is a new type of magnetic material with stable structure, high magnetic permeability, excellent ductility, and good mechanical properties, making FeGa material a focus of attention in the field of sensors and fast, miniaturized high-frequency devices. In 2000, Guruswamy S and others in the United States reported that FeGa alloys have high magnetostrictive properties [10]. Since then, FeGa films have been widely used to build composite magnetoelectric thin film materials and devices [11]. In this work, we report the fabrication of ferromagnetic structures consisting of Fe₇₀Ga₃₀ nano thin films grown on Si/SiO₂ substrates. We found that the resistance behavior of Fe₇₀Ga₃₀ nano thin films with applied voltage was abnormal, indicating that the applied voltage can directly modulate the resistance state of Fe₇₀Ga₃₀ nano thin films. The electric field directly controls the resistance state of the ferromagnetic thin film, that is, the magnetoelectric coupling effect on the metal surface provides new possibilities for the realization of nonvolatile memory.

2. Experimental

Fe₇₀Ga₃₀ magnetic nano thin films of different thicknesses were successfully deposited by ion beam deposition coating on Si/SiO₂ substrates. The nano thin films were deposited under discharge voltage of 65V, acceleration voltage of 250V and beam voltage of 0.5Kv. During the deposition process, argon gas was continuously injected, and the argon gas flow was maintained at 5.6 Sccm. nano thin films with thickness of 2nm, 5nm, 10nm, 15nm and 20nm were deposited respectively. The microstructure of the prepared films was characterized by Grazing incidence

X-ray diffraction (GIXRD, BrookeD8, Advance) and atomic force microscope (AFM, Agilent 5600). Vibration sample magnetometer (VSM, Lake Shore 7404) was used to analyze the magnetic properties of the films. Semiconductor device analyzer B1500A was used to analyze the resistance switching behavior of thin films. Hall effect was measured by physical property measurement system (ppms-9).

3. Results and discussion

Fig.1 shows the grazing incidence XRD diffraction pattern of different thickness $\text{Fe}_{70}\text{Ga}_{30}$ nano thin films. Since the thickness of the films are very thin, we use the grazing incidence method to measure. Grazing incidence XRD eliminates the interference of the film substrate diffraction signal on the diffraction peak of the film. A body-centered cubic structure (bcc) FeGa (110) diffraction peak appeared near 45. When the film thickness is 2nm, no diffraction peak appears. As the film thickness gradually increases to 5 nm, FeGa (110) diffraction peaks begin to appear near 45. As the film thickness continues to increase, 10nm, 15nm, and 20nm samples FeGa (110) diffraction peaks also appeared near 45, indicating that the thin films samples have good crystal orientation growth.

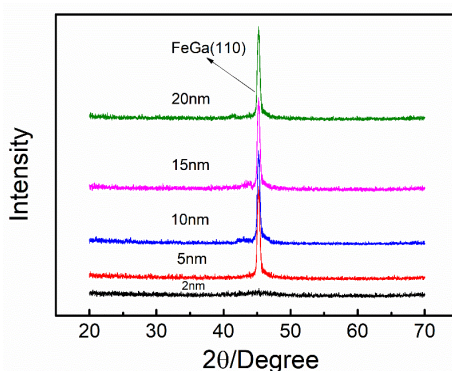


Fig. 1. Grazing incidence XRD patterns for 2nm, 5nm, 10nm, 15nm, and 20nm $\text{Fe}_{70}\text{Ga}_{30}$ nano thin films.

The AFM images of different thickness $\text{Fe}_{70}\text{Ga}_{30}$ nano thin films have been shown in Fig. 2. The change in color over the vertical scale shows the variation in thickness. It can be seen from the comparison of AFM images that although the particle size given by AFM is not real, it can reflect a certain change rule. The nano thin films are composed of uniform small particles. With the increase of thickness, the microscopic surface of the nano thin films become denser and the particles gradually increase.

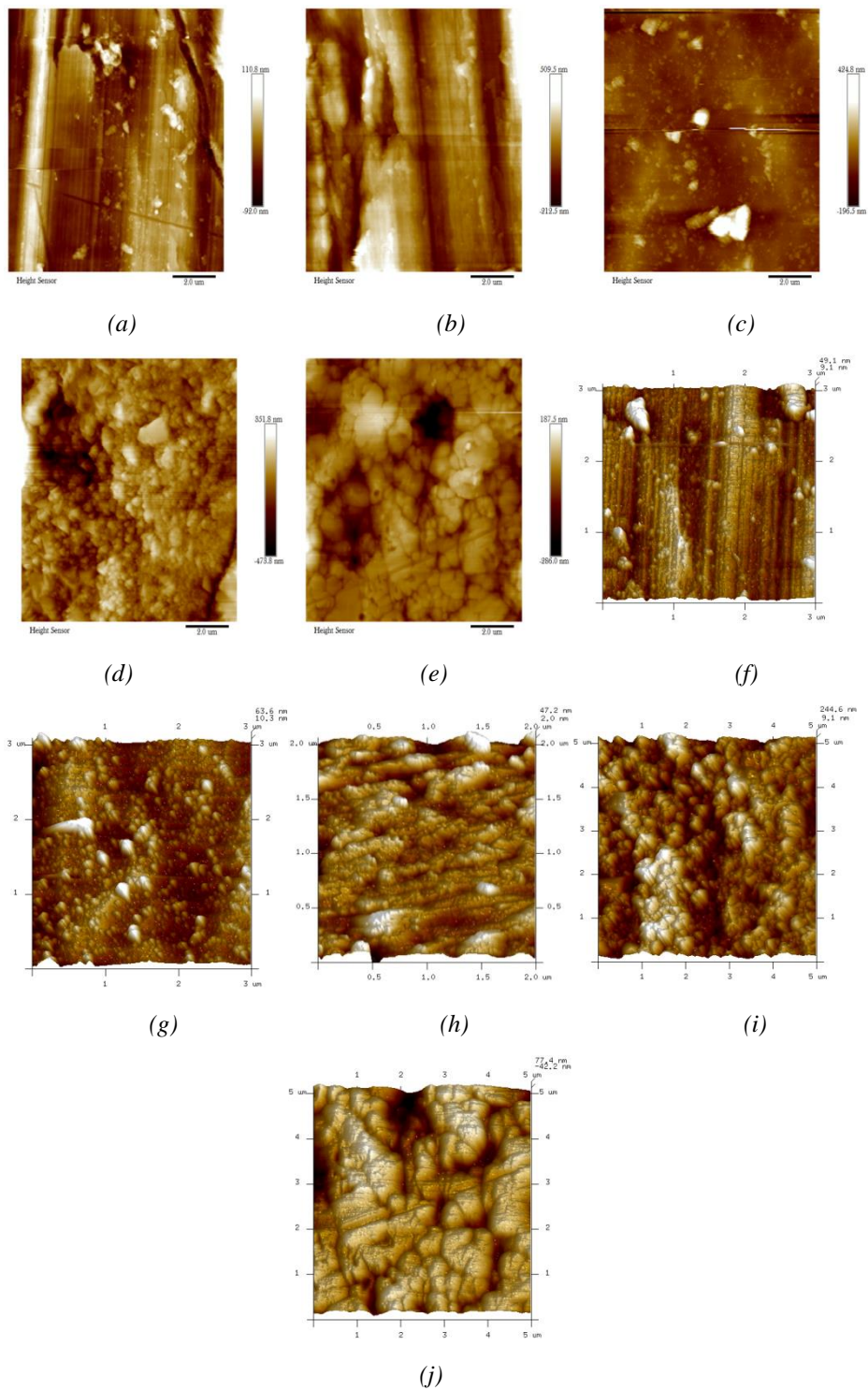


Fig. 2. AFM analysis of 2nm, 5nm, 10nm, 15nm, 20nm $Fe_{70}Ga_{30}$ nano thin films, respectively: (a,b,c,d,e)2D analysis, (f,g,h,i,j)3D analysis.

Fig. 3 shows hysteresis loops for $Fe_{70}Ga_{30}$ nano thin films with thicknesses of 2nm, 5nm, 10nm, 15nm and 20nm. It was found that, with the increase of film thickness, the saturation magnetization intensity gradually increased, and it was about $3 \times 10^{-5} \text{ emu/mm}^3$, $5 \times 10^{-5} \text{ emu/mm}^3$, $7 \times 10^{-5} \text{ emu/mm}^3$, $1 \times 10^{-4} \text{ emu/mm}^3$, $3 \times 10^{-4} \text{ emu/mm}^3$, for 2nm, 5nm, 10nm, 15nm and 20nm $Fe_{70}Ga_{30}$ nano thin films, respectively. $Fe_{70}Ga_{30}$ nano thin films had coercive force

of about 12 Gauss, 35 Gauss, 43 Gauss, 49 Gauss, 57 Gauss, for 5nm, 10nm, 15nm and 20nm thick $\text{Fe}_{65}\text{Co}_{35}$ films, respectively, confirming that the $\text{Fe}_{70}\text{Ga}_{30}$ nano thin films had good soft magnetic characteristics.

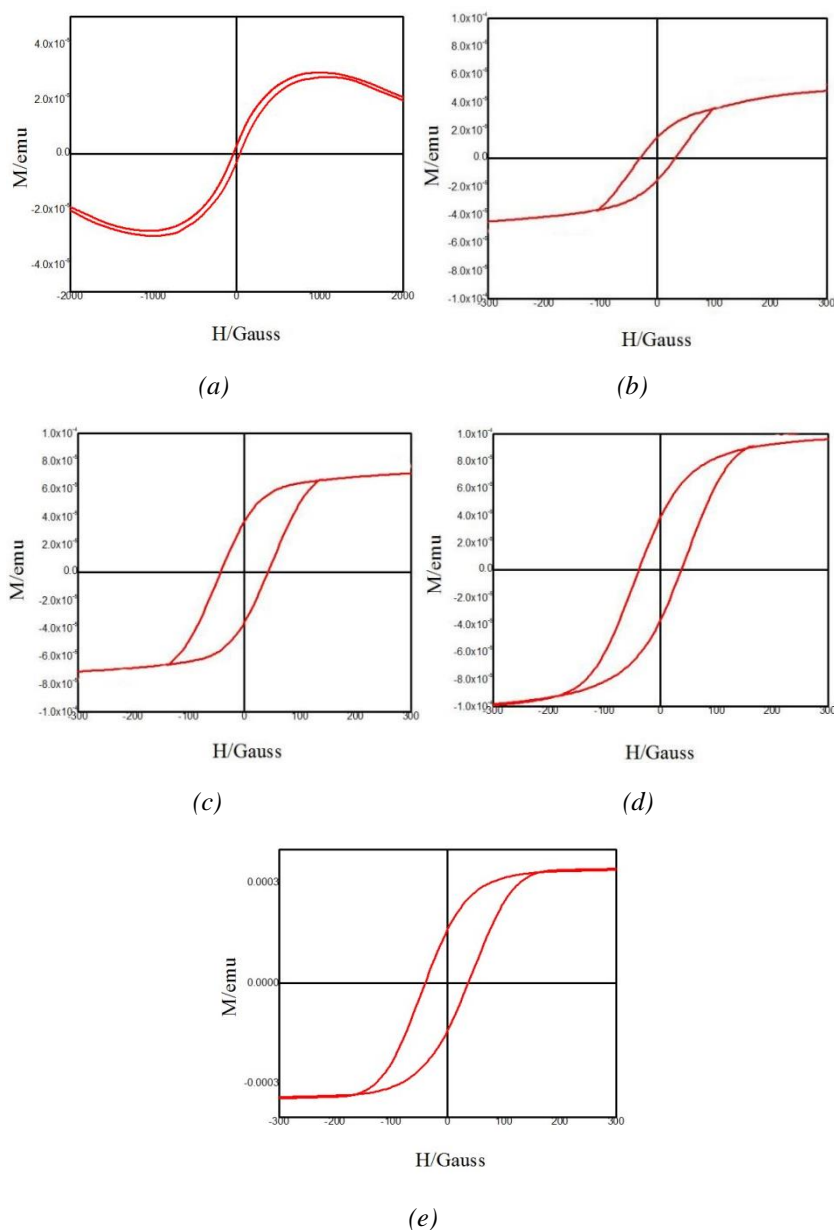


Fig. 3. Magnetization hysteresis loops(a, b, c, d and e) of 2nm, 5nm, 10nm, 15nm, 20nm $\text{Fe}_{70}\text{Ga}_{30}$ nano thin films, respectively

Fig. 4 illustrates the I-V curves of $\text{Fe}_{70}\text{Ga}_{30}$ nano thin films with thickness of 2nm, 5nm, 10nm, 15nm and 20nm. Because the thickness of 2nm thin film is too thin, there is no resistance switching. The current as a function of voltage no longer exhibits a proportional relation behavior, for instance, for the 10nm thick $\text{Fe}_{70}\text{Ga}_{30}$ nano thin films, when the sweep voltage is 150 mV, the current increase steeply from 10 μA to above 110 μA , indicating the presence of low resistance state, and as the sweeping voltage increases to 200 mV, the current decreases sharply from 110 μA

to about 10 μA indicating that the sample was switched to high resistance state, then the current changes substantially proportionally to the voltage. In this regime, the current voltage behavior develops a resistive switching behavior, and it produces more than an order of magnitude change in resistance. Note that, the threshold voltage for the switch of the low resistance state to the high resistance state is increased from 140 to about 300 mV when the films thickness increases from 5nm to 20nm.

The bulk metal material has good conductivity, but when the size of the metal material is reduced to nanometer size, its surface structure is different from that of the bulk metal. The surface structure of the film will form a nano-film with island structure composed of metal clusters. When electrons are transported on the surface of this film, they will be affected by the Coulomb blockade effect, which will cause resistance switching behavior [12].

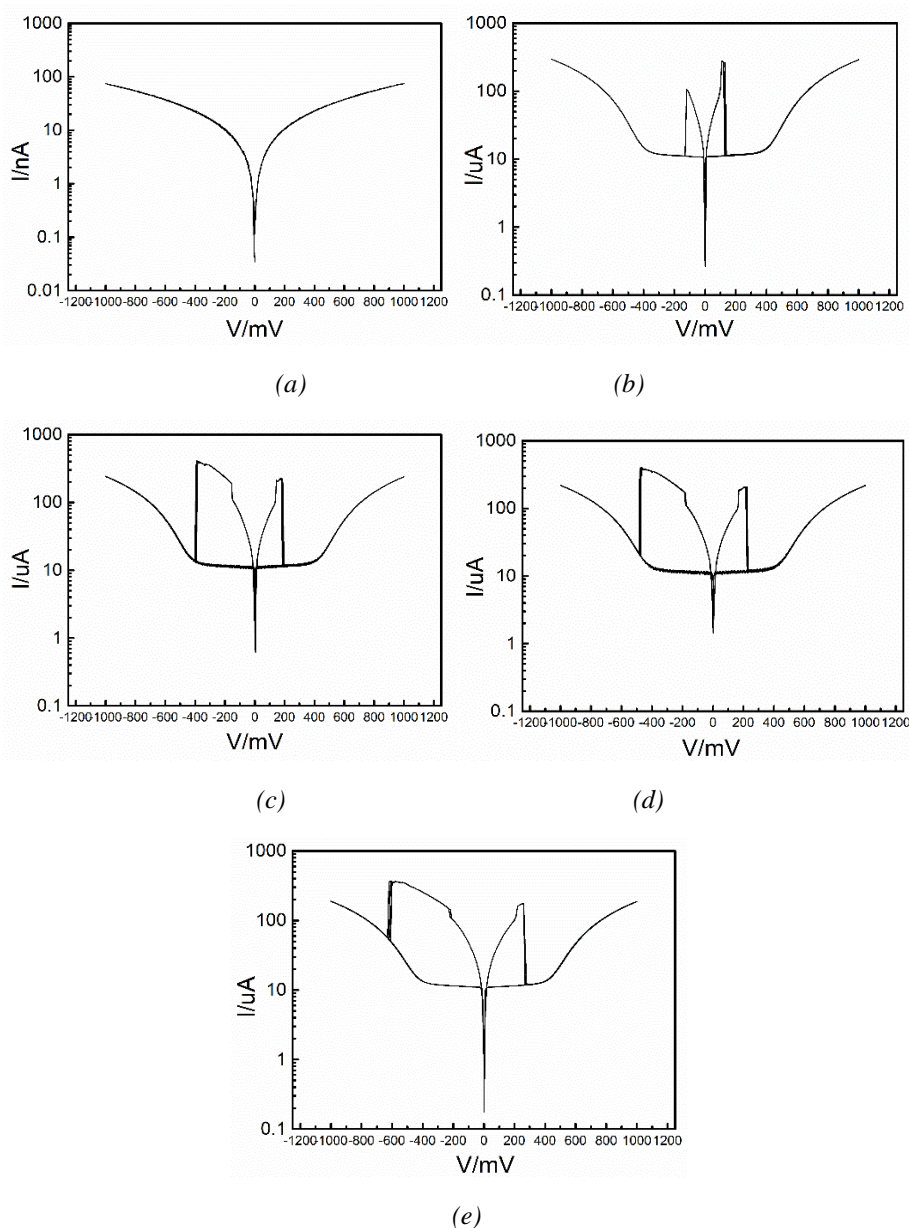


Fig. 4. I - V behaviors (a, b, c, d and e) of 2nm, 5nm, 10nm, 15nm, 20nm $\text{Fe}_{70}\text{Ga}_{30}$ nano thin films, respectively.

Fig. 5 shows the hall resistivity of 5nm, 10nm, 15nm, and 20nm Fe₇₀Ga₃₀ nano thin films at room temperature in relation to the applied magnetic field. 2nm film is too thin to exceed the test range. Anomalous Hall effect is observed for Fe₇₀Ga₃₀ nano thin films. Anomalous Hall resistivity is defined as follows:

$$\rho_{xy} = R_0 B + \mu_0 R_s M \quad (1)$$

R_0 is the normal Hall coefficient, B is the applied magnetic field strength, μ_0 is the vacuum permeability, R_s is the abnormal Hall coefficient, and M is the spontaneous polarization strength of the ferromagnetic material. The Hall to hold, R_{Hall} , is given by the sum of the ordinary Hall effect (OHE) due to the Lorentz force and the anomalous Hall effect (AHE) originating from asymmetric scattering in the presence of magnetization [13]. It can be seen from Fig. 5 that hall resistance rises rapidly with the increase of magnetic field intensity, which could be caused by the increase of the vertical component of magnetization. When the magnetic field is low, abnormal hall effect dominates. When the magnetization M reaches saturation, hall resistivity increases linearly with a small slope and approaches saturation, which is caused by the normal hall effect [14]. As the thickness of the Fe₇₀Ga₃₀ nano thin films increase from 5nm to 20nm, we can find that the slope becomes larger at low fields, indicating that the anomalous Hall effect becomes larger and larger.

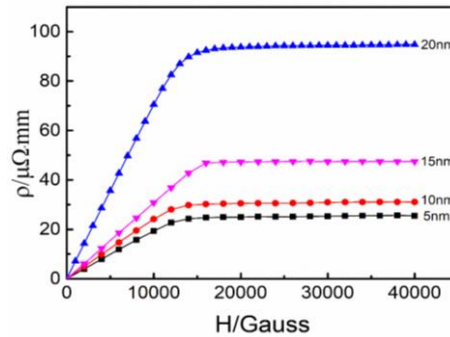


Fig. 5. Hall resistivity of 5nm, 10nm, 15nm, and 20nm Fe₇₀Ga₃₀ nano thin films.

The research shows that in ferromagnetic metallic systems, the change in magnetism is often related to the carrier density [15]. Due to the anomalous Hall effect on the surface of Fe₇₀Ga₃₀ nano thin films, the surface carrier density of Fe₇₀Ga₃₀ nano thin films changed when Hall effect test was performed resulting in magnetic switching. Therefore, the electric field modulate the carrier density and electron arrangement of the Fe₇₀Ga₃₀ nano thin films, thereby realizing the modulation of the macroscopic magnetic properties by the electric field.

4. Conclusions

In summary, Fe₇₀Ga₃₀ magnetic nano thin films of different thicknesses were successfully deposited by ion beam deposition coating on Si/SiO₂ substrates. Under the action of electric field, resistance switching and magnetic switching occurred on the surface of Fe₇₀Ga₃₀ nano thin films. The electric field modulated transport behaviors could be attributed to the density of the itinerant electrons in metals. The electric field directly controls the resistance state of the ferromagnetic nan thin films, that is, the magnetoelectric coupling effect on the metal surface provides new possibilities for the realization of nonvolatile memory.

Acknowledgments

This work is supported by the National Natural Science Foundation of China.

References

- [1] D. Meier, J. Seidel, A. Cano, K. Delaney, Y. Kumagai, M. Mostovoy, N. A. Spaldin, R. Ramesh, M. Fiebig, *Nature Materials* **11**, 284 (2012).
- [2] Weisheit, S. Fahler, A. Marty, Y. Souche, C. Poinignon, D. Givord, *Science* **315**(5810), 349 (2007).
- [3] A. Jaiswal, K. Roy, *Scientific Reports* **7**, 39793 (2017).
- [4] K. Eid, H. Kurt, W. P. Pratt, J. Bass, Miura, N. Yamazoe, *Phys. Rev. B* **70**(10), 100411 (2004).
- [5] S. Ueda, M. Mizuguchi, M. Tsujikawa, M. Shirai, *Science and Technology of Advanced Material* **20**(1), 796 (2019).
- [6] A. M. Chornous, Yu. O. Shkurdoda, V. B. Loboda, Yurii Shabelnyk, *European Physical Journal Plus* **132**(1), 11327 (2017).
- [7] Ben Wortmann, Dennis van Vorden, Paul Graf, Roberto Robles, *Nano Letters* **16**(1), 528 (2015).
- [8] T. Nozaki, Y. Shiota, S. Miwa, S. Murakami, F. Bonell, S. Ishibashi, H. Kubota, K. Yakushiji, T. Saruya, A. Fukushima, S. Yuasa, T. Shinjo, Y. Suzuki, *Nature Physics* **8**, 491 (2012).
- [9] S. Li, *Journal of Alloys and Compounds* **448**(1), 73 (2008).
- [10] P. Mungsantisuk, R. P. Corson, S. Guruswamy, *Journal of Applied Physics* **98**(12), 123907 (2006).
- [11] W. N. Eerenstein, N. D. Mathur, J. F. Scott, *Nature* **442**(7104), 759 (2006).
- [12] S. Kubatkin, A. V. Danilov, A. L. Bogdanov, H. Olin, *Applied Physics Letters* **73**(24), 3604 (1998).
- [13] N. A. Sinitsyn, *Journal of Physics: Condensed Matter* **13**, 202 (2008).
- [14] F. Matsukura, D. Chiba, T. Omiya, E. Abe, T. Dietl, Y. Ohno, K. Ohtani, H. Ohno, *Physica E* **12**, 351 (2002).
- [15] D. Anh Tuan, D. Duc Dung, V. T. Son, Y. Shin, S. Cho, *Journal of Applied Physics* **111**(7), 50 (2012).